OFFICE OF NAVAL RESEARCH

Contract NOOO14-92J-1590

Technical Report No. CWRU/DMS/TR-47

Diffusion of Polyphenylene Oxide and Polystyrene using Variable Angle ATR

by

Robert A. Shick, Jack L. Koenig and Hatsuo Ishida

Department of Macromolecular Science
Case Western Reserve University
Cleveland, Ohio 44106-7202

February, 1993

Principal Investigator
Hatsuo Ishida
(216) 368-4285

NAME OF PERFORMING ORGANIZATION	6b OFFICE SYMBOL (If applicable)	7a NAME OF MONITORING ORGANIZATION
se Western Reserve University		Office of Naval Research
ADDRESS (City, State, and ZIP Code) partment of Macromolecular Science eveland, Ohio 44106-1712		7b. ADDRESS (City, State, and ZIP Code) 800 North Quincy St. Arlington, VA 22217
NAME OF FUNDING/SPONSORING ORGANIZATION fice of Naval Research	8b OFFICE SYMBOL (If applicable)	9. PROCUREMENT INSTRUMENT IDENTIFICATION NUMBER
ADDRESS (City, State, and ZIP Code) 0 North Quincy Street lington, VA 22217		10 SOURCE OF FUNDING NUMBERS PROGRAM ELEMENT NO. / PROJECT NO. / TASK NO. / WORK UNIT ACCESSION NO

TITLE (Include Security Classification)

ffusion of Polyphenylene Oxide and Polystyrene using Variable Angle ATR

PERSONAL AUTHOR(S)

bert A. Shick, Jack L. Koenig, Hatsuo Ishida

TYPE OF REPORT	13b TIME COVERED	14 DATE OF REPORT (Year, Month, Day)	15. PAGE COUNT
chnical Report	FROM _____ TO _____		

SUPPLEMENTARY NOTATION

bmitted to Macromolecules

COSATI CODES			18 SUBJECT TERMS (Continue on reverse if necessary and identify by block number)
FIELD	GROUP	SUB-GROUP	

ABSTRACT (Continue on reverse if necessary and identify by block number)

gration in the polyphenylene oxide - polystyrene system has been investigated using a riable angle internal reflection spectroscopic technique. Particular attention has been voted to the condition where the PPO is glassy and the PS is in the molten state. For is case, the overall diffusion has been observed to be Fickian, however there are also me non-Fickian characteristics.

DISTRIBUTION/AVAILABILITY OF ABSTRACT	21. ABSTRACT SECURITY CLASSIFICATION	
☒ UNCLASSIFIED/UNLIMITED ☐ SAME AS RPT. ☐ DTIC USERS	unclassified	
NAME OF RESPONSIBLE INDIVIDUAL Dr. Kenneth Wynne	22b. TELEPHONE (Include Area Code) (202) 696-4410	22c. OFFICE SYMBOL

Diffusion of Polyphenylene Oxide and Polystyrene using Variable Angle ATR

Robert A. Shick, Jack L. Koenig and Hatsuo Ishida

Department of Macromolecular Science

Case Western Reserve University

Cleveland, Ohio 44106

Abstract:

Migration in the polyphenylene oxide - polystyrene system has been investigated using a variable angle internal reflection spectroscopic technique. Particular attention has been devoted to the condition where the PPO is glassy and the PS is in the molten state. For this case, the overall diffusion has been observed to be Fickian, however there are also some non-Fickian characteristics.

Introduction:

Compatible polymer pairs are quite rare, especially ones which are compatible across their entire composition range. This is because the combinatorial entropy of mixing of polymers is quite small, scaling as N^{-1}, where N is the degree of polymerization, therefore the mutual diffusion of a polymer pair is dependent upon segmental interaction, i.e. a negative Flory interaction coefficient, χ.[1] One of the classic polymer pairs which is completely compatible for any composition is polystyrene (PS) and poly(2,6-dimethyl-1,4-phenylene oxide) (PPO). Blends of PS and PPO have been shown to exhibit a single glass transition intermediate to the pure materials, indicating a rheologically compatible blend.[2] However, the glass transition determined using different techniques yields slightly different values, for example dielectric

measurements, differential scanning calorimetry (DSC), and dynamic mechanical measurements all give different glass transition temperatures. This has been rationalized by recalling that each technique probes a different effective volume, so that the different results imply then the PPO-PS system is not compatible on the segmental level, however the degree of mixing does extend to very small volumes.[3]

The segmental interaction which is responsible for the compatibility of PS-PPO was the subject of an infrared investigation by Wellinghoff et al.[4] They concluded that there exists a strong interaction between the phenyl ring of the PS and the phenylene ring of the PPO, which in turn induces a change in the conformation of the PPO chain. More recently, in a solid state nuclear magnetic resonance (NMR) investigation, supporting evidence has been found for this mechanism.[5] These researchers found that a strong π-π interaction occurs between the aromatic rings of the PS and PPO, and this is the most direct reason for the miscibility of these blends.

While the study of the miscibility of PPO and PS has been relatively straight-forward, the investigation of their inter-diffusion has been much more difficult. This is because it is necessary for more exotic techniques to be employed to determine profile distributions, usually neutron scattering or an ion-beam analysis method such as forward recoil spectrometry are used. Both techniques require that the species to be measured are deuterated. These techniques can provide very accurate profiles, however it is necessary to change the nature of the sample to allow investigation. The advantage of using an infrared spectroscopic technique is that the material's own vibrations can be used to probe the profiles without any change to the sample and may be performed with common laboratory instrumentation. The disadvantage is that the spatial resolution of the internal reflection technique is inferior to the ion beam techniques. Therefore, the different techniques can provide complementary information, and a combination of techniques is recommended. One recent study has attempted to investigate mutual diffusion of different polymers using attenuated total reflection (ATR) fourier transform infrared spectroscopy (FTIR).[6] Their study yielded a diffusion coefficient about one order of magnitude

below that of the well-accepted ion beam experiments of Green et al.[7] for the inter-diffusion of atactic polystyrenes, which they were trying to reproduce with their ATR technique. The virtue of their experiment is that it made use of common laboratory instrumentation, however, their low diffusion coefficient is likely due to the lack of detailed consideration of the optical theory governing their experiment which should be applied in the analysis of their data. The theoretical developments allowing accurate depth profiling of stratified layers has recently been put forth by Shick et al.[8] It is the intent of this paper to show how ATR can disclose the profiles of inter-diffusion of PPO and PS, a compatible polymer pair.

Experimental:

Germanium hemi-cylinders were obtained from Harrick Scientific. These hemi-cylinders were used in a variable angle attachment from Perkin Elmer. The incident angle was varied from 24° to 57° which was the full range allowed by the attachment. Sixteen individual spectra were collected in addition to the corresponding reference spectra. A wire grid polarizer was used to control the incident polarization. The spectra were taken with a Fourier transform infrared spectrophotometer (Bomem DA-3). Spectra were taken under vacuum (0.5 torr) and a liquid-nitrogen-cooled, narrow bandpass mercury-cadmium-telluride (MCT) detector was used with a specific detectivity D* of 2.1×10^{10} cm $Hz^{1/2}/W$. Happ-Genzel apodization was used and the resolution reported is after apodization. Typically, 2000 scans were co-added with a resolution of 4 cm^{-1} unless otherwise stated. The aperture was set to 5mm.

Thin films of PPO were deposited onto the hemi-cylinders by spin coating from solution in spectrophotometric grade chloroform obtained from Aldrich, which was used as received. The PPO, from Polysciences, Inc., had a weight average molecular weight (M_w = 44,300), and polydispersity (M_w/M_n = 2.45) as measured using gel permeation chromatography (GPC) based on PS standards. The PPO was used as received. Spin coating was performed by depositing 0.2 ml of 60 mg/ml solution on the germanium hemi-cylinder, then spinning at 3000 rpm for 2

minutes. Next, the film was held at 180 °C for 12 hours to assure that all traces of the chloroform had been completely removed. The film thickness was determined to be 0.63 μm using a Dektak IID profilometer from Sloan Technologies equipped with a 25 μm diameter stylus, and this thickness was reproducible to within 0.02 μm between different films. The PS, also from Polysciences, Inc., had a weight average molecular weight (M_w = 273,200) and a polydispersity (M_w/M_n = 5.0) using GPC based on PS standards. The PS was used as received. A separate film about 200 μm thick was cast from a chloroform solution. This film was dried at 50 °C for two hours, then 90 °C for two hours, 140 °C for 36 hours, and finally 180 °C for 2 hours. It was necessary to take greater precautions in drying the PS because the films were significantly thicker than those of the PPO. Both the coated germanium and the PS film were heated to 180 °C. The germanium was then pressed onto the PS film, and the system was allowed to remain at 180 °C for 30 minutes. Subsequent diffusion was achieved by heating the germanium/polymer bi-layer to 230 °C under an argon purge for 30, 60, and 120 minutes cumulatively.

Samples for the determination of the optical constants were prepared by casting films of approximately 200 μm thick from chloroform solution onto the germanium hemi-cylinder. These samples were then subjected to the same drying regimen as the PS films.

The non-linear least squares estimation of the inverse Laplace transform is done using a Simplex algorithm which is a component of a statistics package, Systat®, from Systat Inc. Spectral simulation[9] and Kramers-Kronig analysis[10] were done using programs developed in our laboratory and were written in Fortran77 on a MicroVAX II with a VMS operating system.

DSC was performed on a Perkin Elmer DSC 7. The scans were run at 20 °C/min and the data are reported from the second heating cycle. The measured glass transition (Tg) for PS was 105 °C, and for PPO was 210 °C. Both samples appeared completely amorphous.

Results:

A description of the Perkin Elmer variable angle attachment and the procedure used to calibrate the incident angle has been discussed in a previous paper.[11] When placing a substrate on the germanium hemi-cylinder which is sufficiently thick such that the evanescent field is completely extinguished within that layer, it is possible to calculate the optical constants, n and k, using Kramers-Kronig analysis. For this experiment, s and p-polarization were used at several angles of incidence for comparison. The resulting optical constants for PPO are shown in Figure 1 and for PS are shown in Figure 2 assuming a limiting refractive index of 1.52. At this point, it is possible to make an interesting comparison to illustrate the interaction of the PS and PPO in a compatible blend. It is possible to simulate the optical constants for the case of a 50 % PPO-PS blend from the individual optical constants. This method inherently assumes that there is no interaction between the phases. Note that this method makes use of the additivity of dielectric constants.[12] The complex dielectric constant is the square of the complex refractive index for dielectric materials, where the magnetic permeability is unity.[13]

$$\hat{\varepsilon} = \hat{n}^2 \qquad (1)$$

Where a "^" indicates a complex quantity, $\hat{\varepsilon}$, is the complex dielectric constant and the complex refractive index is defined by $\hat{n} = n + ik$. Once the theoretical, non-interactive result is obtained for the 50% blend, it can be compared to the actual optical constants for the 50% blend. By subtracting out the non-interactive prediction, the interactive components of the spectra will be highlighted. This series is shown for the extinction coefficients, k, in Figure 3. To minimize the effect of any errors in the comparison, the spectra were scaled to the prominent aromatic ether band at 1190 cm^{-1} before subtraction, so that only relative differences will be displayed. The most profound effect is seen for the aromatic ether band around 1190 cm^{-1}. In fact the appearance of a new band, indicated in the figure, presumably arising from the interactions is found at 1180 cm^{-1}. This was seen as a change in peak shape in the work of Wellinghoff et al., and was interpreted as a change in the PPO chain conformation.[4] In addition, discrepancies arising from interaction can be seen for the aryl C-H wag for both the PPO at 858 cm^{-1} and the

PS at 907 cm^{-1}. The effect is slightly more pronounced for the PPO aryl C-H wag than for the corresponding PS band, involving a 7.5% and 5% change respectively from the non-interacting prediction. The changes in the 858 cm^{-1} band are also in accordance with the results of Wellinghoff et al. and in agreement with the phenyl ring interaction proposed by both Wellinghoff et al.[4] and Feng et al.[5] It should be remarked that the effects of interaction were also observed for bands at 956, 1019, 1303, 1378, 1421, 1453, 1467, and 1596 cm^{-1}. When visible, the interactive effects account for about 5% of the overall band intensity; so while the effects are visible, they are not prominent. However, the effects are much more noticeable by subtracting out the non-interactive component, as opposed to noticing band shape distortions as in the case of Wellinghoff et al. Note that the negative peaks in Figure 3 indicate a shift in the center of gravity of the respective bands, leading to a derivative-type band shape.

It is the intent of this paper to present depth profile information concerning the inter-diffusion of PPO and PS. To this end it is desirable to use bands which are negligibly affected by the interaction of these components. Certainly the C-H stretching region is a good choice. The level of interaction, as mentioned previously, is on the order of 5% of the overall band intensity, so even when it occurs it will have a minor effect on the calculated profiles. These effects are most obvious for the stronger bands simply from overall intensity considerations, and it is the stronger bands which are least appropriate for depth profile determination.[8] It has also been shown in a previous study that there is less error in the profile determination if p-polarization is used during the experiment, therefore this study will also employ p-polarization.[9] It should be noted that use of an iterative technique, using refined estimates based on calculated extinction coefficient values, was used in that paper. This was valid for step profiles, however this practice can seriously influence the profile estimation for the general type which will be used in this manuscript. Therefore, it is recommended that iteration not be used routinely, and it will not be used here. The details and virtues of the analysis method are discussed in those papers, however it is based on an inverse Laplace transform and can theoretically be used with either

polarization. Spectra are recorded at various angles over the range of the attachment and then each unique band is fit to determine a concentration profile. Perhaps the need for such an analysis method can be clarified with the following example. Traditionally, when some qualitative depth information is desired with ATR, the band intensities are plotted as a function of the reciprocal of the decay constant, where γ is the decay coefficient:[14]

$$\gamma = \frac{2\pi n_1 \sqrt{\sin^2 \theta_1 - \left(\frac{n_2}{n_1}\right)^2}}{\lambda} \qquad (2)$$

Here, θ is the incident angle, n_1 and n_2 are the refractive indices of the internal reflection element and the substrate respectively, and λ is the wavelength of radiation under consideration. The parameter, γ, has units of reciprocal length so its inverse is often referred to as the "depth of penetration," but physically it refers to the distance where the field intensity has fallen to 1/e of its original intensity for a transparent substrate, since γ is actually an exponential decay coefficient. For the germanium-PPO-PS sandwich structure which has been held at 180 °C, the absorptance, (A=1-R), of the aryl C-H wag is plotted for PS (907 cm^{-1}) and PPO (858 cm^{-1}) as a function of $1/\gamma$ in Figure 4. Given that the PS film is pressed onto the PPO film at 180 °C, 30 °C below the Tg of the PPO, it is reasonable to expect that the PPO absorptance would decline at greater depths and the PS would increase in a commensurate manner. Perhaps they would even represent a step function. In any case, it is obvious that the presentation of the data as shown in Figure 4 does not lead to any intuitive interpretation. About all that can be said is that as the depth increases so does to total absorptance, with no hint as to the overall profile.

A significant improvement to this approach is to use the method which has been alluded to which requires an inverse Laplace transform. Actually, it is more convenient to hypothesize a profile, take the Laplace transform, and fit the data in the Laplace domain, since this requires the least data. It is appropriate to comment on some of the limitations of the technique from the outset. Of particular concern in the subject of uniqueness. When a possible function for the profile is considered, it is usually considered over all real space, and when the Laplace transform

of this function is taken analytically, its transform is valid over all Laplace space. However, the data are over a finite range in Laplace space, so assuming a functional form essentially fixes the Laplace function to which the data is fit. There are indicators as to the goodness of fit, however it is impossible to resolve fine details with competing functions which offer similar goodness of fit, so it is important to consider only physically reasonable profiles and then to compare overall behavior. It is very difficult to discriminate between two very similar profiles. In this regard, it is also important to consider systematic changes in a profile rather than isolated profiles. Even with such limitations it is possible to achieve some insight as to the distribution of components.

The Perkin Elmer attachment allows only 16 different angles to be probed due to the limited angular accuracy, so it is desirable to be as frugal as possible when introducing adjustable parameters due to the rather limited degrees of freedom. This restriction can be relaxed with a more accurate reflection attachment. There is one additional complication in that a hyperbolic tangent or a sum of error functions normally describes the profile for Fickian diffusion.[15,16] However, there is no analytic solution for the Laplace transform of these functions, and it is prohibitive to solve it numerically. It is possible to conceive of a series of lines which could serve as a very close approximation to the hyperbolic tangent (tanh) profile, as shown in a schematic in Figure 5. Here, the composition profile is shown to increase with distance, however it could just as easily be decreasing. The major advantage of the tanh profile is that it can be described with 3 adjustable parameters while the series of lines requires 4 adjustable parameters. Fitting 16 data points to a curve involving 4 adjustable parameters is problematic, there are concerns as to statistical significance as well as many local minima due to experimental error. However, it is possible to reliably fit the data to 3 adjustable parameters, so various simplifications are made to reduce the general 4 parameter model, then the overall fits are compared to decide on the most probable profile.

This method actually yields extinction coefficient profiles, however since only unique bands are being analyzed, the extinction coefficients may be normalized by their pure values to

give a composition profile. Consider a linear profile which remains constant at k_i until some distance z_i, which then ascends or descends until z_f where it remains constant at k_f. These parameters are also shown schematically in Figure 5. The Laplace transform of this profile is shown in equation (3).

$$\mathcal{L}\{k(z)\} = \frac{(k_i - k_f)\left(e^{sz_i} - e^{sz_f}\right)}{s^2(z_f - z_i)e^{s(z_i+z_f)}} + \frac{k_i}{s} \qquad (3)$$

The Laplace variable, s, is equal to twice the decay coefficient, so it is twice equation (2). Equation (3) was then simplified in the following ways: for one set of approximations, k_i was set to zero for increasing profiles and k_f was set to zero for decreasing profiles. This set is particularly liberal for the decreasing profile because it is possible to fall to k_f only at $z \rightarrow$ infinity, and since a range from 0 to 1.5 μm is all that is feasible for the current experimental technique[11], the numerical restrictions are very mild. For another set of approximations, z_i was set to zero, which allows an increasing profile the same flexibility as the decreasing profile was afforded in the previous approximation. Lastly, a step profile was considered where $z_i = z_f$ and either k_i or k_f were zero depending on whether the step was from the germanium surface or if there was some gap. This is the crudest measure of whether a profile is increasing or decreasing, but it is still far more effective than plotting as a function of $1/\gamma$, recalling Figure 4.

To check the feasibility of the approach for these profiles, synthetic spectra based on classical dispersion theory were used. This method has been detailed in a previous paper.[8] This afforded error free model spectra which could then be combined to allow different compositions of two separate spectra to be generated using the principles of dielectric additivity, recalling equation (1). The synthetic composition profile was determined using a hyperbolic tangent (tanh), with realistic depths. Two bands were considered, each representing a different component, one centered at 1500 cm^{-1} and the other at 1000 cm^{-1}, each with an extinction coefficient of 0.05. Because the simulation requires discrete stratified layers, the continuous tanh profile was approximated by 75 discrete steps, each 20 nm in width. The composition of each layer could be varied independently. The Reflectance spectra was then determined for angles of

incidence between 26 and 64° with half degree increments using s-polarization. The absorptance data which was generated was then fit to the simplification of equation (3) to determine the error of the approach. For convenience, the composition which is decreasing from the optically dense medium will be called "A," and the composition which is increasing will be called "B." The composition profile which has been simulated as well as the best fit profiles are shown in Figure 6. It can be seen that the center of the profile is well estimated, however the slope is somewhat over estimated. The decreasing profile, "A," tends to overestimate the slope more severely than the increasing profile, "B." The composition must add to unity, so the composition of "A" determined by the increasing profile is just 1-"B."

The first step was to apply the step function simply to see if the profile was increasing or decreasing from the surface. For the sample heated to 180 °C, every band that was clearly associated with the PS showed that there was some distance before the PS began. Likewise, every band associated with the PPO showed that the PPO composition began directly at the hemi-cylinder and then tapered off over distance. Interestingly, for common bands, or bands which were severely overlapping, the profile started at the hemi-cylinder and continued to infinity. These results were of course expected, however it was reassuring to observe. The composition profiles which will be displayed are principally from the first set of approximations, although all of the results were corroborated with the second set. Of course, the profiles were also consistent with the step profiles. This method yields an extinction coefficient profile, k(z), so normalization by the respective extinction coefficient of the pure material gives a composition profile, c(z).

The sandwich structure, germanium-PPO-PS which was in contact at 180 °C for 30 minutes gives the PS composition profile shown in Figure 7. This profile is quite expected since the profilometer indicated that the PPO layer was about 0.63 μm. The slight extra distance could be accounted for by thickness variations or by experimental error. The average thickness, i.e. the midpoint for the profile, obtained from this measurement is 0.74 μm (std 0.08 μm). The slope is

also quite high at 16.3 (std 2.6), indicating a relatively sharp step in the PS profile. These results suggest that the PS is in good contact with the PPO layer. However, the profile for the PPO layer, shown in Figure 8, is somewhat unexpected. This seems to indicate that the PPO has inter-diffused into the PS layer, even though 180 °C is still 30 °C below the Tg for PPO. This is well within the experimental limits of the technique. In a previous study[11] films of polymethylmethacrylate (PMMA) were cast onto germanium to form a step profile. If the same approximated hyperbolic profile is fit to that data, the slope is generally much steeper, typically around 100, which is much steeper than even the PS profile shown in Figure 7. Diffusion in the glassy state is not typical, and this behavior will be investigated further. There may be some incorporation of PS into the PPO which is beyond the simple profile to which the data is being fit. In a separate sandwich sample which had been heated to 140 °C, the PPO layer remained a step function of appropriate thickness, although the contact with the PS was poor. The migration of the PPO into the PS was also observed in a separate sample which had been held at 190 °C for one hour. The results shown in Figures 7 and 8 imply density fluctuations along the z-direction, most likely due to the simplistic model profile to which the data are being fit. It is known that PPO and PS exhibit a negative excess volume of mixing, however this change is quite minor compared with the range of density under current consideration.[17] Since density fluctuations are unlikely, a more probable cause is that the three parameter model does not allow the flexibility to accurately represent the existing situation, and the apparent density fluctuations are simply a manifestation of this approximation. A more reasonable profile is shown in Figure 9, although it is somewhat conjecture since it is beyond the current measurement sensitivity of the technique. What has been done is that an average composition has been calculated for both materials using the bands shown in Figures 7 and 8, and wherever the local composition does not add to unity, the difference is split between the two components to adjust to this constraint.

The composition profile after subjecting the sandwich structure to 230 °C for 30 minutes is shown for PS in Figure 10. The center of the diffusion profile is seen to shift from 0.74 μm to

0.21 μm (std 0.08 μm). In addition, the slope has decreased from 16.3 to 4.6 (std 1.4), and an effective diffusion coefficient can be calculated just from the change in slope. If this is done, a value of 0.2 x 10^{-13} cm^2/s is obtained for the PS diffusing into the PPO. This is within the range of diffusion coefficients measured for deuterated PS and PPO inter-diffusion, 10^{-13} cm^2/s measured at 206 °C, which was measured using forward recoil spectrometry, an ion-beam analysis technique.[18] In their study they were looking at very slight composition differences, nominally 50% with less than 1% difference in composition, since their objective was to determine a mutual diffusion coefficient. The composition profile for the PPO under the same conditions is shown in Figure 11, it should be noted that both curves are shown, but they are completely overlapping. The PPO has completely diffused into the PS such that no slope is observable. The level of PPO has dropped to 22%. If the total composition is again constrained to unity, and the differences are split evenly between the two components, the profile shown in Figure 12 is observed. When the sandwich structure is placed at 230 °C for longer periods of time, the PS profile remains essentially unchanged, and PPO profile remains constant but the height drops slightly with increasing time.

The migration of PPO and PS below the glass transition has recently been observed using Rutherford backscattering.[19] Here the PPO and PS were held in contact at 184 °C for various times, then the films were stained with bromine. The bromine has a large Rutherford cross-section and can bond directly with about one third of the PPO repeats. The profile can then be measured by bombarding the film with helium ions and observing the radial scattering intensity. Migration of species below the glass transition was also observed in a PS-PVME (polyvinylmethylether) blend using neutron reflection spectroscopy.[20] The latter authors proposed the following mechanism. When two polymers are miscible, the high mobility, low Tg, component penetrates into the low mobility, high Tg, component. This diffusion should not be Fickian, rather it should be similar to case II diffusion which is typical for a good solvent penetrating into a glassy polymer. Dissolution of the high-Tg component should occur rapidly

after penetration. Therefore, it would be expected for a front to move into the high-Tg component.

For the system currently under investigation, the simplistic linear profiles are unable to capture the complexity of this phenomenon in a completely quantitative manner, due principally to the limited range and accuracy of the variable angle attachment. An additional constraint is that the field decay coefficient, γ, never approaches infinity, so there is a minimum distance which can be determined. Below this distance, any profile which conserves area is a possible solution. For the current experimental configuration, this limit is around 0.3 μm. The PS layer, the back layer, is less affected by this since, for the most part, its volume is beyond this limit and we will concern ourselves with these profiles. This was also seen using the simulated results shown in Figure 6., where the estimates of the back layer more closely approximated the actual profile. A new sample is prepared, this time placing the thick PS film in contact with the PPO surface for 30 minutes at 160 °C, then for 30 minutes at 180 °C. The PS profiles shown by the bands at 3081, 3059, and 3026 cm^{-1} are shown in Figure 12. The sub-Tg transport of the PS, and hence the PPO, is clearly evident as the system is held at 180 °C for 1 and 8 hours respectively. If the overall process was Fickian, then the mid-point displacement would be linear with the square root of time, which is shown in Figure 13 using an average midpoint. These results agree with the results of Composto et al.[19] who also observed $t^{1/2}$ behavior with this system at several different temperatures below the PPO Tg. The PS influx into the PPO layer seems to be moving as a relatively steep front, shown in Figure 12. Although the 3 parameter profiles pre-dispose this type of behavior, the high slope may also be a result of the non-Fickian processes alluded to by Suaer et al.[20]

The driving force for the migration below the PPO Tg is likely the specific interactions between the phases. The excess Gibbs free energy of mixing per segment can be represented by the following regular solution model:

$$\Delta G_{mix}^{ex} = \chi \phi_A \phi_B k_B T \qquad (4)$$

Where χ is the Flory interaction parameter, ϕ is the volume fraction of both components, k_B is the Boltzmann constant, and T is the temperature. From this it can be seen that everywhere χ is negative, the free energy is a driving force which allows mixing, only the mobility is constraining. It has been observed that χ = -0.033 for dilute PS in glassy PPO.[21] In addition, Composto[18] has determined that χ=0.145-78/T, although it was measured above the Tg of the blends, it presumably indicates that χ is negative for temperatures below 265 °C. The mobility of the PS is apparently sufficient to the free energy driving force to occur with sufficiently long periods.

Some of the results are decidedly Fickian, namely the $t^{1/2}$ dependence on the midpoint migration, although they do tend to show some non-Fickian characteristics, namely that the PS is advancing with a steeper slope than the PPO is receding when observing the individual components. The latter behavior is reminiscent of Case II diffusion, where a PS front is migrating toward the hemi-cylinder surface with a relatively steep slope. Furthermore, in the literature it has been assumed that deuterated profile studies would correspond well to their non-deuterated counter-parts, however since the techniques which have been used previously require deuteration this hypothesis has gone unchallenged. Indeed, Cowey has recently remarked that in his systems, deuteration greatly influences the phase behavior, significantly increasing the interactions between polymers.[22] This can be seen to some extent in the interaction coefficient, χ, where it has been determined to be χ=0.121-77.9/T for dilute deuterated-PPO in PS.[18] Comparing this result to that of Composto's best fit values for a non-deuterated system, χ=0.145-78/T, indicates that indeed the deuterated system has more interaction. Such an effect might change the character of diffusion, and the current method of investigation might lend some insight as to the magnitude of those changes since it presumably would work equally well with deuterated or non-deuterated components.

Conclusions:

The interaction and diffusion of PPO and PS has been investigated using a variable angle internal reflection infrared technique. Interactions between the polymers were clearly observed by subtracting out the non-interactive components of the infrared spectra. The migration of PPO and PS was seen to occur even at 30 °C below the glass transition temperature of the PPO. The migration of PS toward the germanium hemi-cylinder and into the PPO-rich phase proceeded with the migration of PPO. Diffusion of the PPO into the PS was rapid above the glass transition, and had reached a steady state value in less than 30 minutes at 230 °C. The change in slope accompanying this migration above the PPO Tg could be fit to a pseudo-Fickian diffusion coefficient, which is in the range of those calculated for deuterated PPO-PS systems investigated by other methods. The migration of the composition midpoint below the PPO Tg proceeded linearly with $t^{1/2}$ which is an indication that the sub-Tg diffusion is Fickian, albeit with some non-Fickian characteristics.

Acknowledgments:

This work was in part sponsored by the Office of Naval Research.

References:

1. P.G. de Gennes, *J. Chem. Phys.*, **72**, 4756 (1980).

2. C. Bouton, V. Arrondel, V. Rey, Ph. Sergot, J.L. Manguin, B. Jasse, and L. Monnerie, *Polymer*, **30**, 1414 (1989).

3. W.M. Prest, R.S. Porter, *J. Polym. Sci.: A-2*, **10**, 1639 (1972).

4. S.T. Wellinghoff, J.L. Koenig, and E. Baer, *J. Polym. Sci.: Polym. Phys.*, **15**, 1913 (1977).

5. H. Feng, Z. Feng, H. Ruan, and L. Shen, *Macromol.*, **25**, 5981 (1992).

6. J. Van Alsten and S. Lustig, *Macromol.*, **25**, 5069 (1992).

7. P.F. Green, P.J. Mills, J. Palmstrom, J.W. Mayer, and E.J. Kramer, *Phys. Rev. Lett.*, **53**, 2145 (1984).

8. R.A. Shick, J.L. Koenig, and H. Ishida, *Appl. Spectrosc.*, (theory, accepted).

9. K. Yamamoto, A. Masui, and H. Ishida, *Phys. Rev. B*, (submitted)

10. K. Yamamoto, A. Masui, and H. Ishida, *Appl. Optics*, (submitted)

11. R.A Shick, J.L. Koenig, and H. Ishida, *Appl. Spectrosc.*, (experimental, accepted).

12. I.F. Chang, S.S. Mitra, J.N. Plendl, and L.C. Mansur, *Phys. Stat. Sol.*, **28**, 663 (1968).

13. F. Wooten, "Optical Properties of Solids," Academic Press, New York, 1972.

14. N.J. Harrick, *J. Opt. Soc. Am.*, **55**, 851 (1965).

15. K. Binder, *J. Chem. Phys.*, **79**, 6387 (1983).

16. L. Leibler, *Macromol.*, **15**, 1283 (1982).

17. H. Hopfenberg, V. Stannett, and G. Folk, *Polym. Eng. Sci.*, **15**, 261 (1975).

18. R.J. Composto, J.W. Mayer, and E.J. Kramer, *Phys. Rev. Lett.*, **57**, 1312 (1986).

19. R.J. Composto and E.J. Kramer, *J. Mater. Sci.*, **26**, 2815 (1991).

20. B. Sauer and D. Walsh, *Macromol.*, **24**, 5948 (1991).

21. A. Maconnachie, R. Kambour, D. White, S. Rostami, and D. Walsh, *Macromol.*, **17**, 2645 (1984).

References (cont):

22. J. Cowie, in an address during a Symposia honoring Robert Simha, held at Case Western Reserve University, Cleveland, Ohio (1992).

List of Figures:

Figure 10: Composition profile of PS for 230 °C after 30 minutes.

Figure 11: Composition profile of PPO for 230 °C after 30 minutes.

Figure 12: Composition profile of PS at 180 °C after 30 minutes (a), 1 hour (b) and 8 hours (c).

Figure 13: The average PS composition midpoint displacement at 180 °C as a function of $t^{1/2}$.

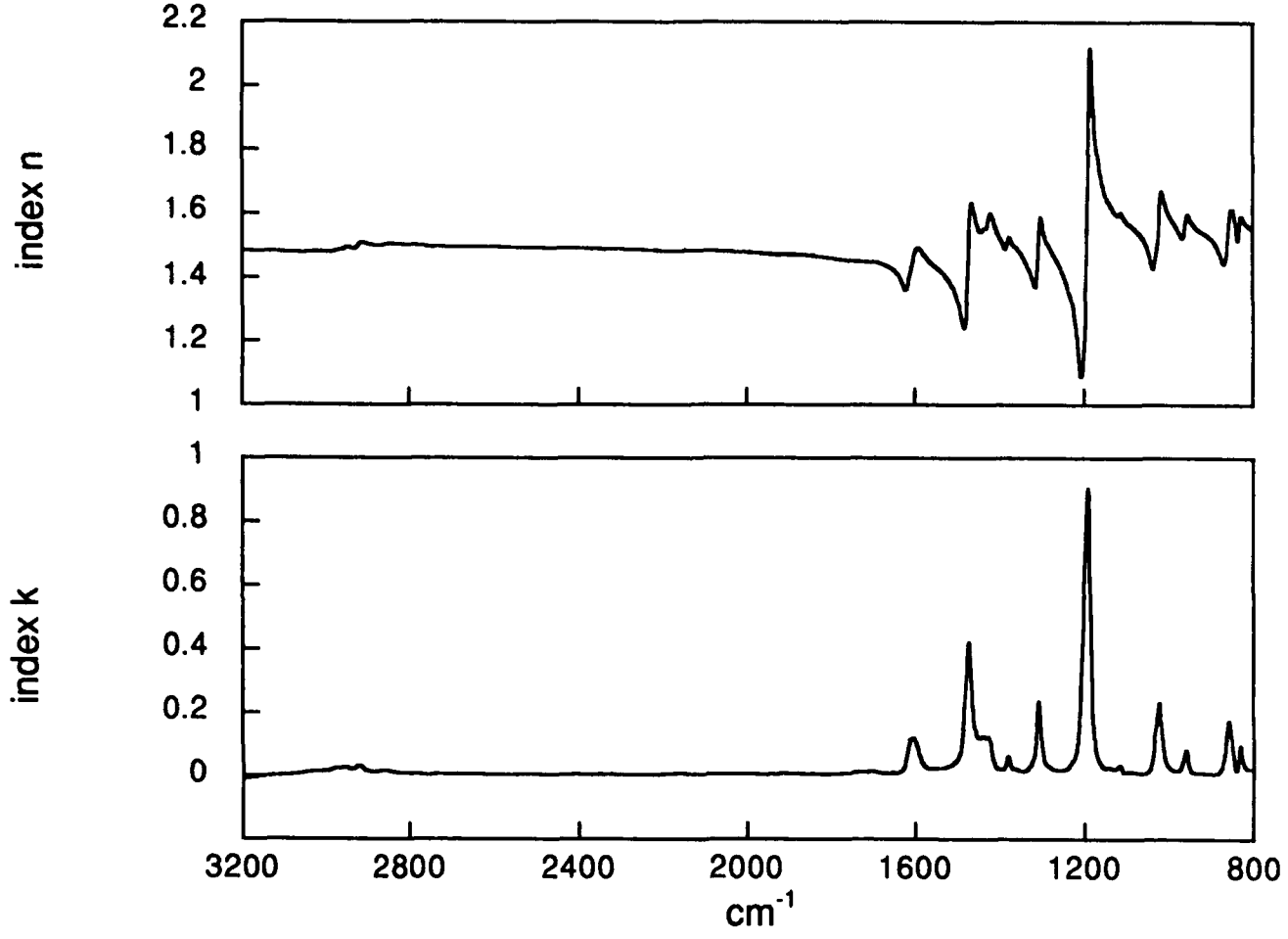
index n
2.2
2
1.8
1.6
1.4
1.2
1
index k
1
0.8
0.6
0.4
0.2
0
3200
2800
2400
2000
1600
1200
800
cm-1

Figure 1

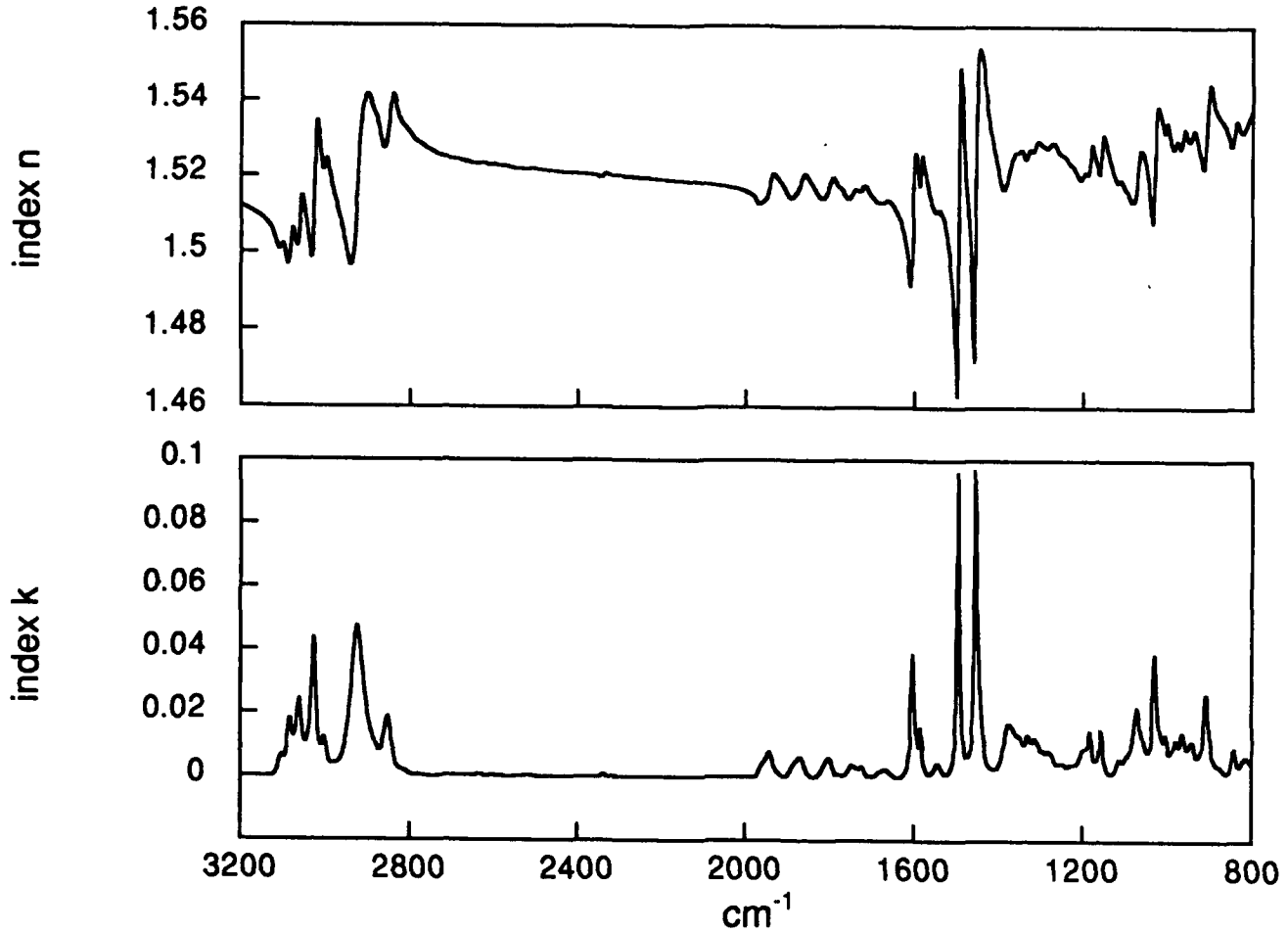
index n
1.56
1.54
1.52
1.5
1.48
1.46
index k
0.1
0.08
0.06
0.04
0.02
0
3200
2800
2400
2000
1600
1200
800
cm-1

Figure 2

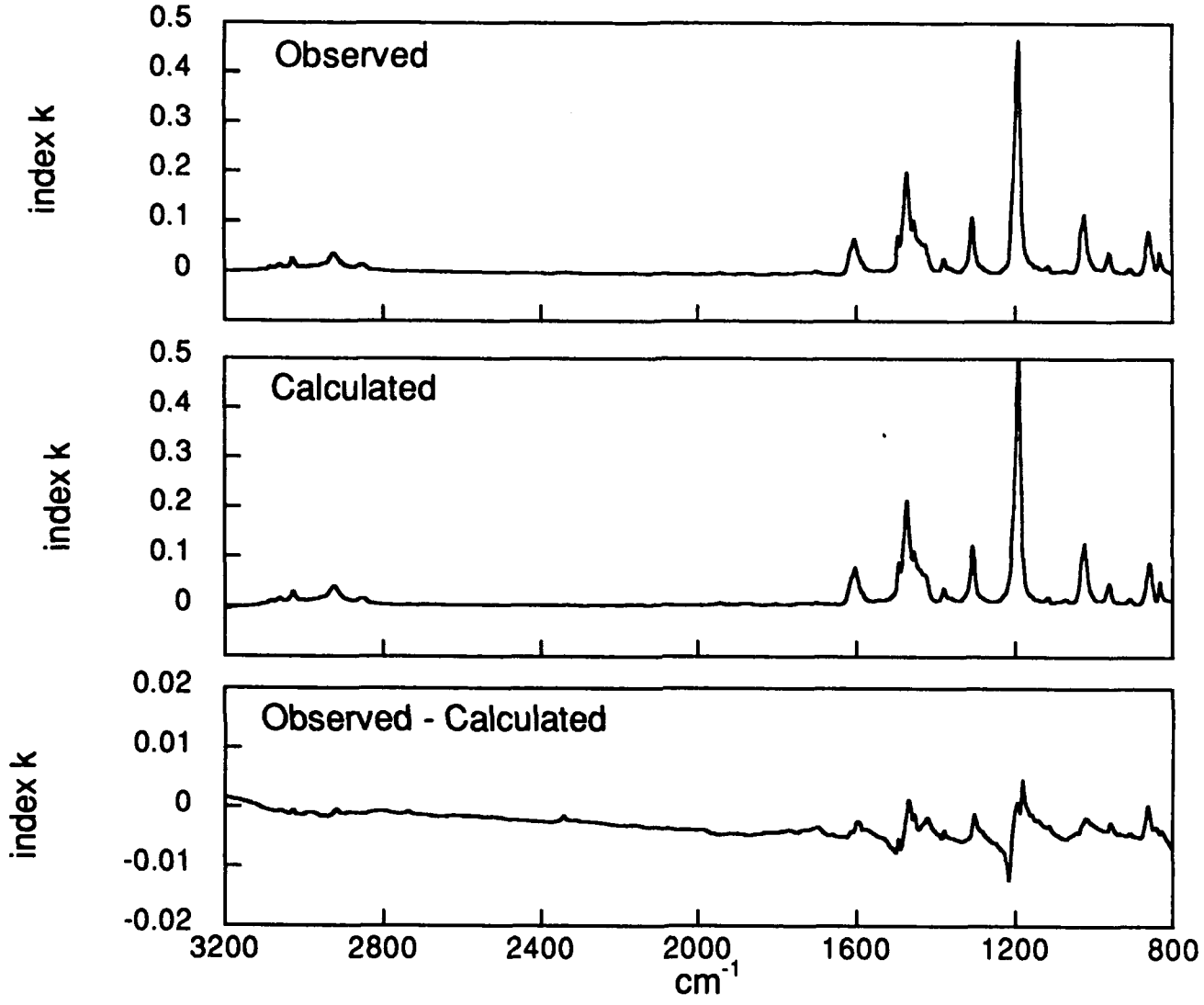
Observed
Calculated
Observed - Calculated
index k
0.5
0.4
0.3
0.2
0.1
0
0.02
0.01
-0.01
-0.02
3200
2800
2400
2000
1600
1200
800
cm-1

Figure 3

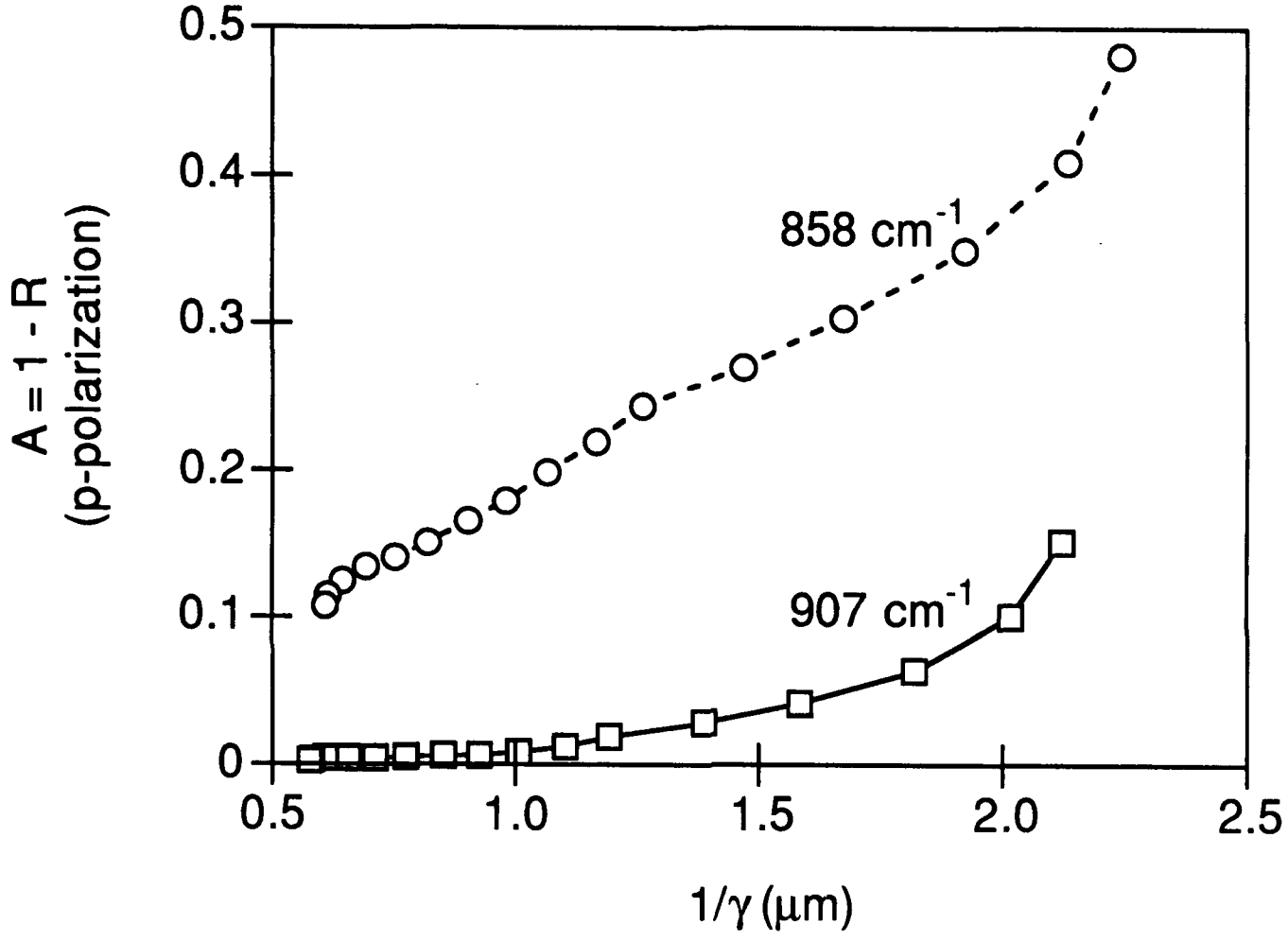
0.5
0.4
0.3
0.2
0.1
0
A = 1 - R
(p-polarization)
858 cm-1
907 cm-1
0.5
1.0
1.5
2.0
2.5
1/γ (μm)

Figure 4

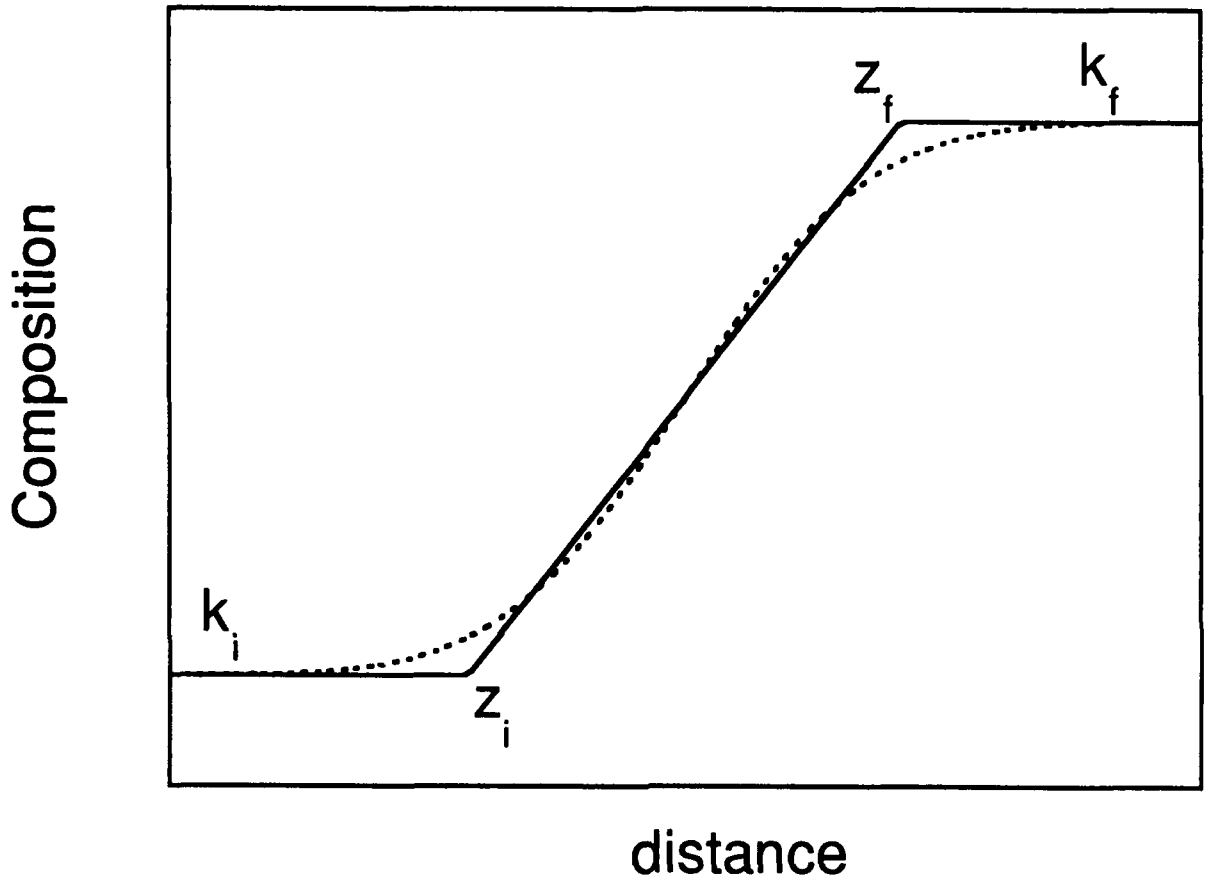

Figure 5

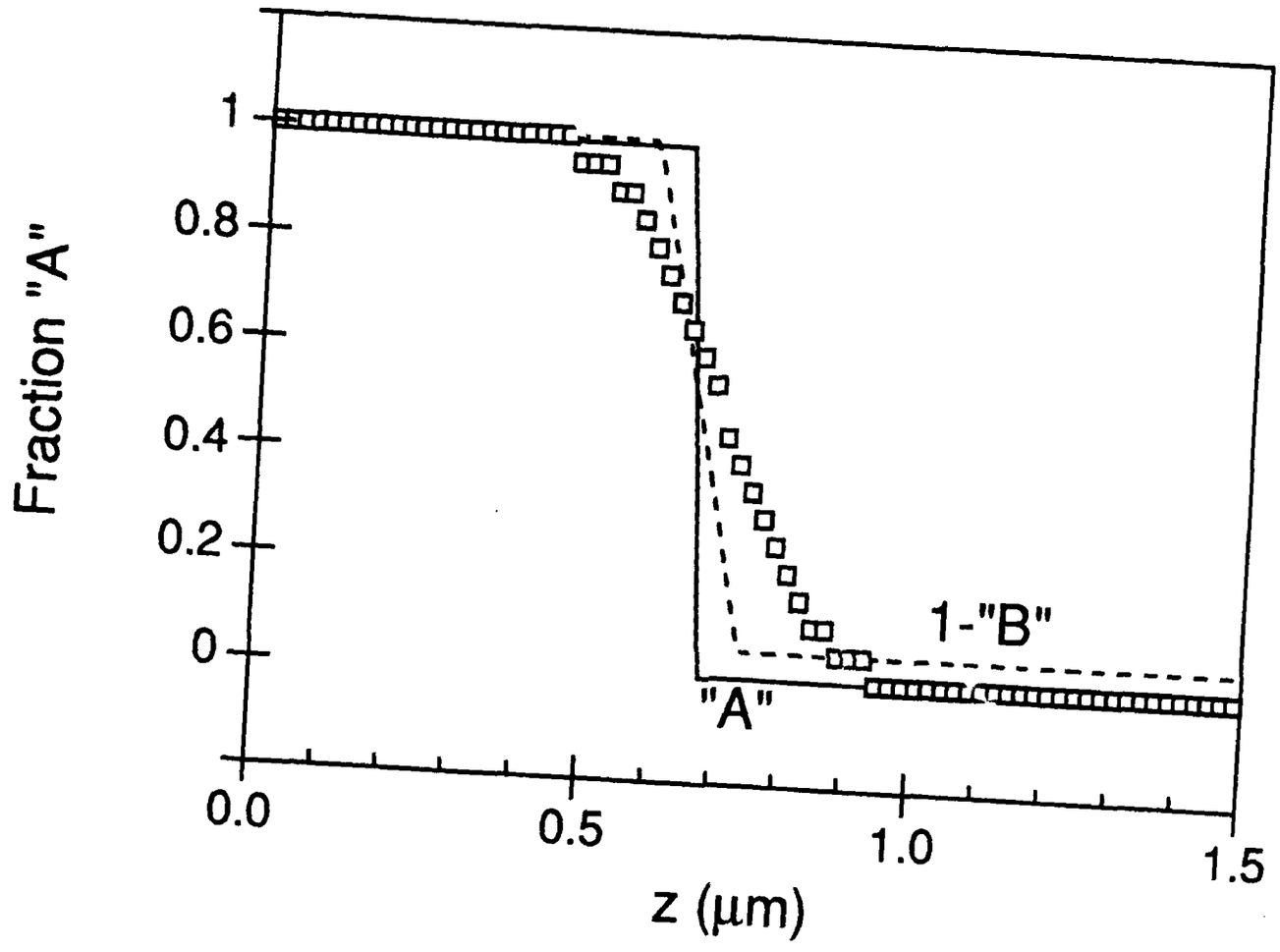

Figure 6

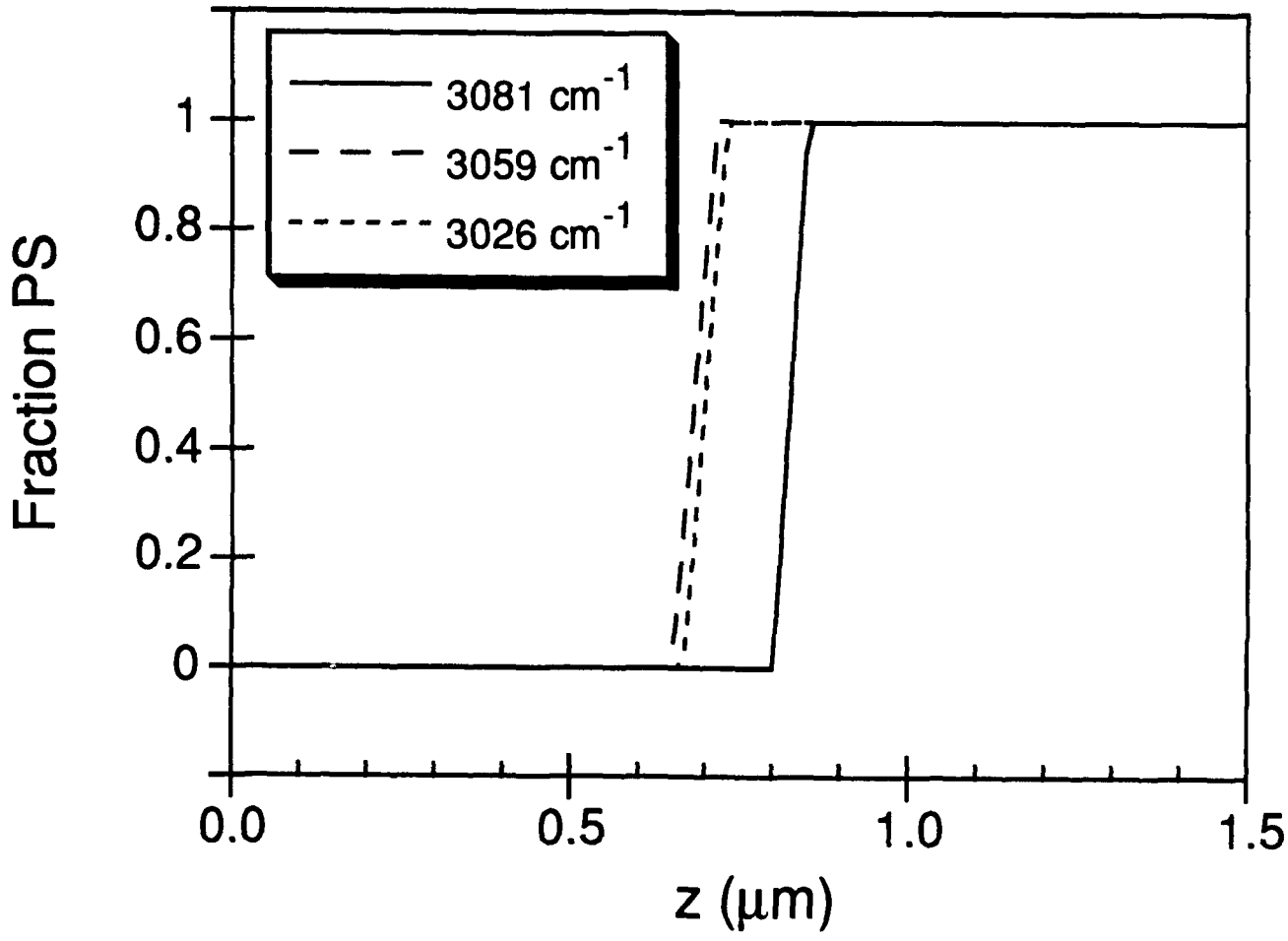
3081 cm-1
3059 cm-1
3026 cm-1
Fraction PS
1
0.8
0.6
0.4
0.2
0
0.0
0.5
1.0
1.5
z (μm)

Figure 7

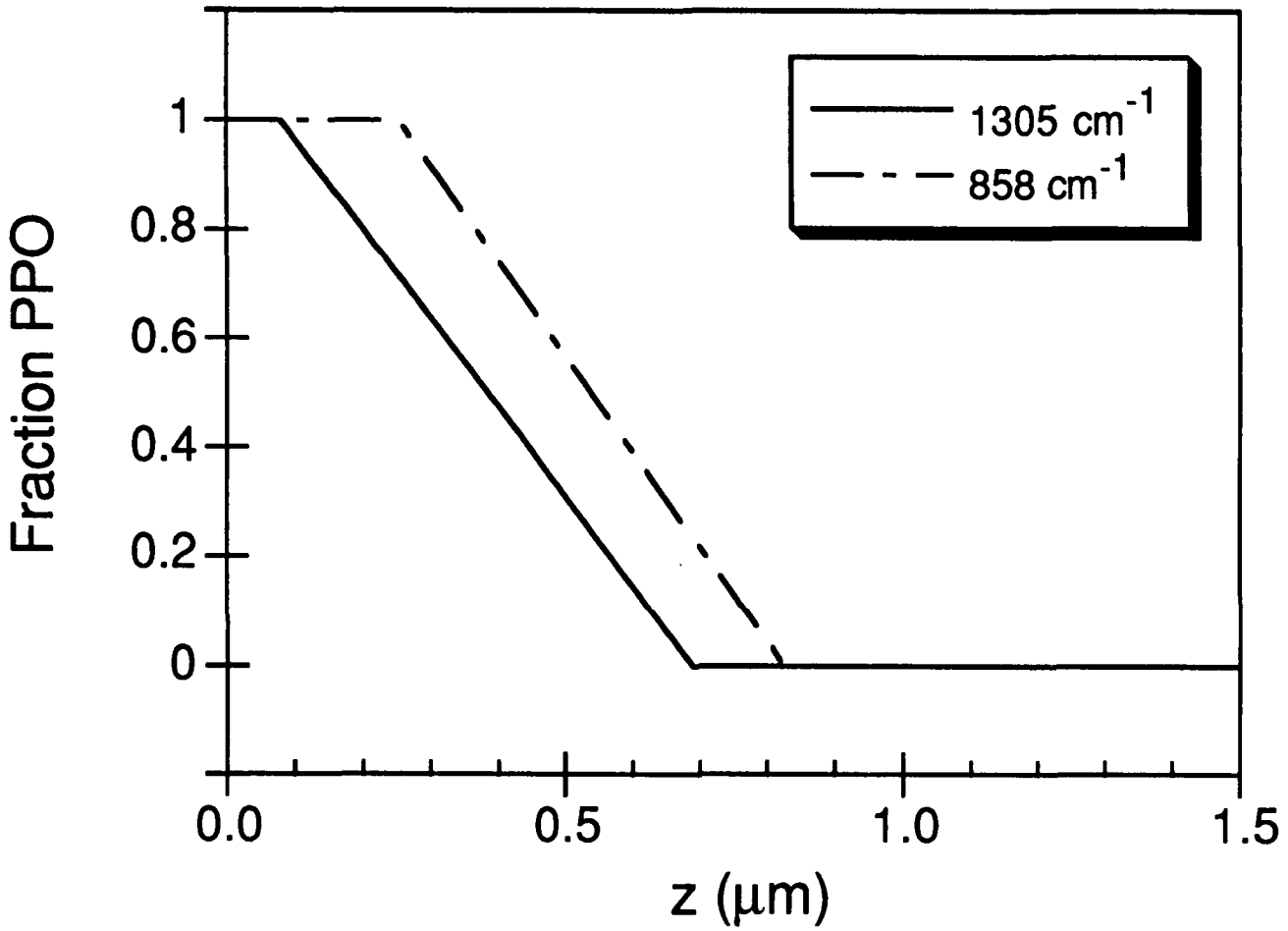

Figure 8

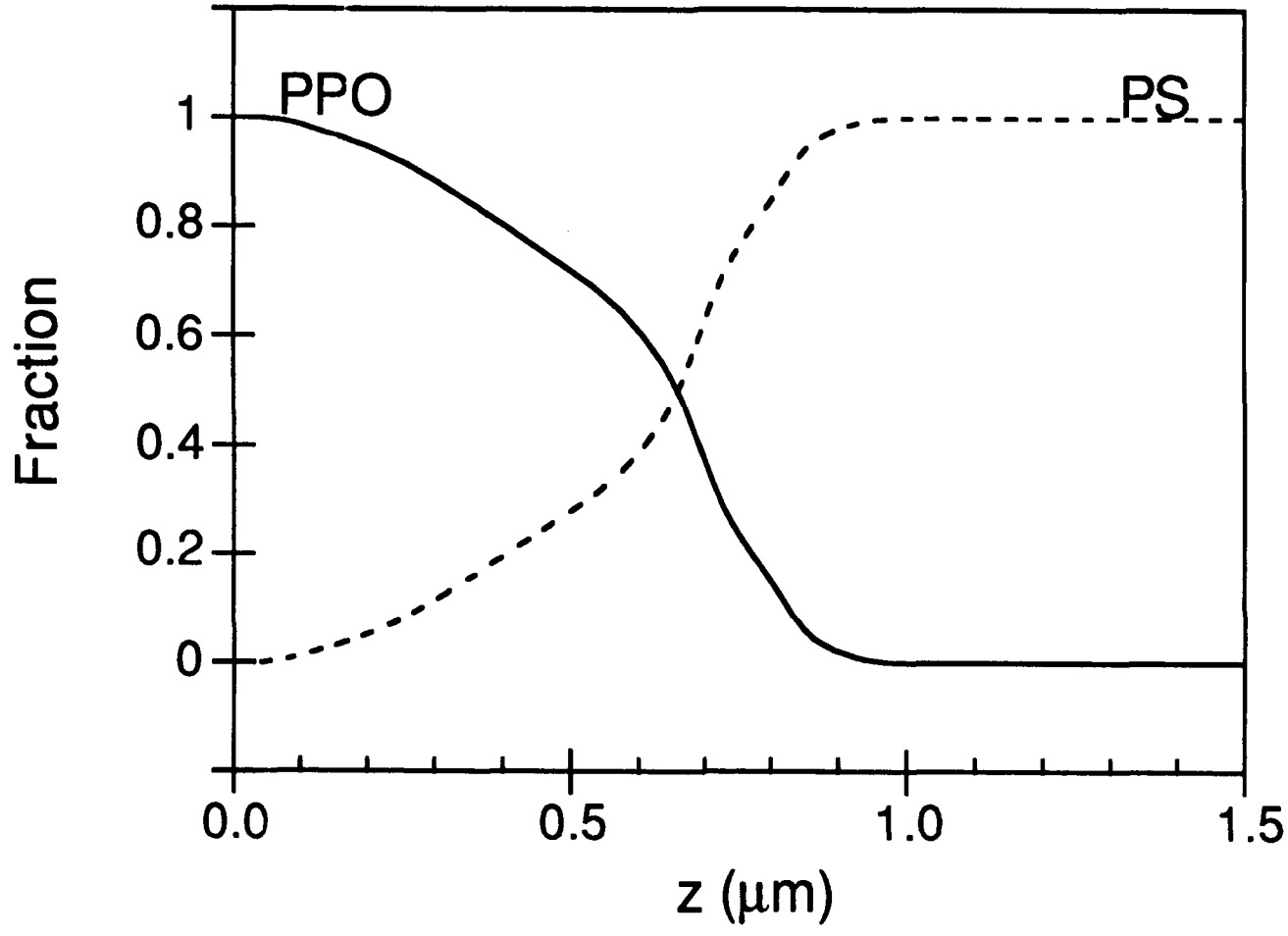

Figure 9

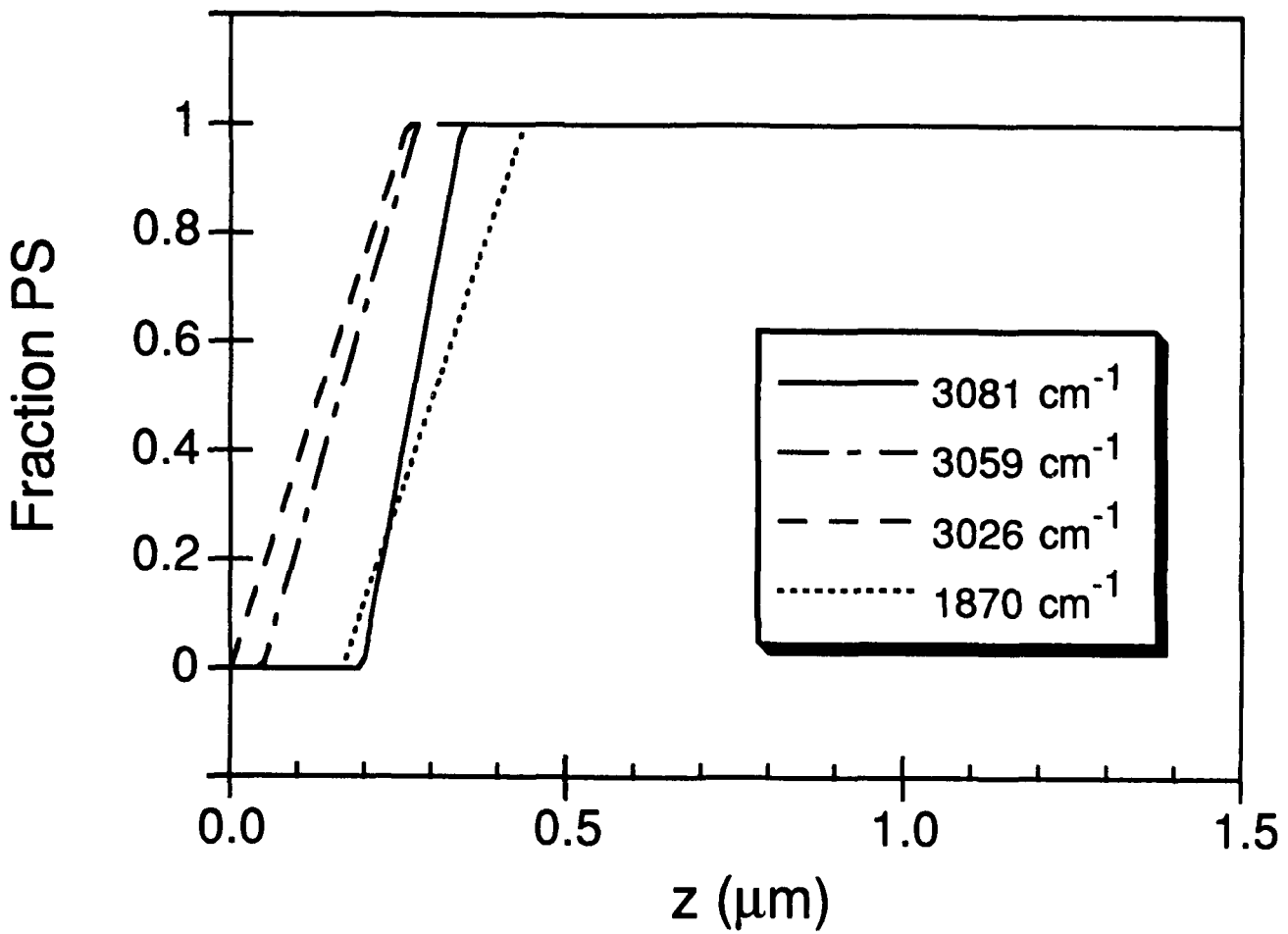
Fraction PS
1
0.8
0.6
0.4
0.2
0
0.0
0.5
1.0
1.5
z (μm)
3081 cm-1
3059 cm-1
3026 cm-1
1870 cm-1

Figure 10

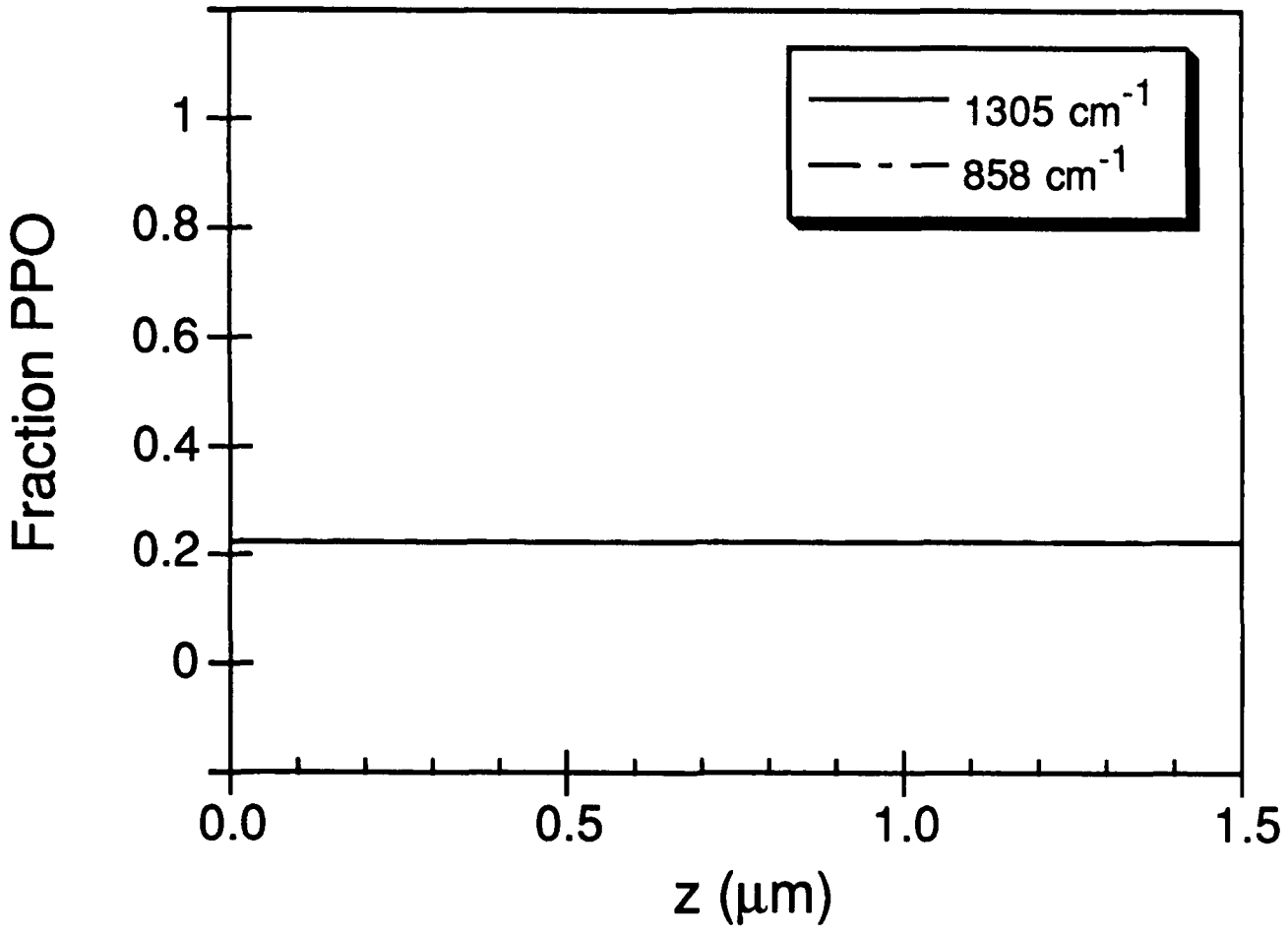

Figure 11

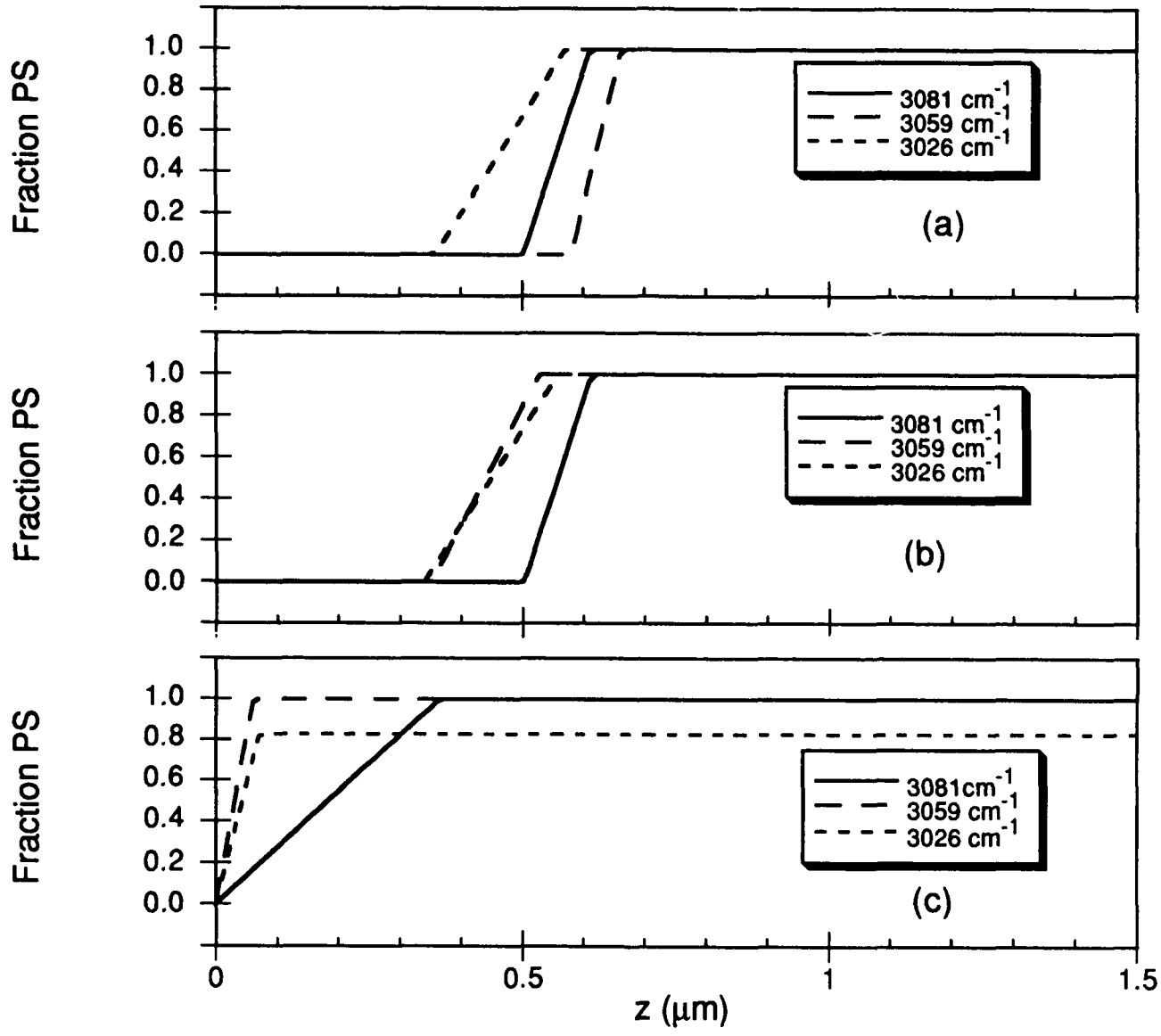
Fraction PS
1.0
0.8
0.6
0.4
0.2
0.0
3081 cm-1
3059 cm-1
3026 cm-1
(a)
(b)
(c)
0
0.5
1
1.5
z (μm)

Figure 12

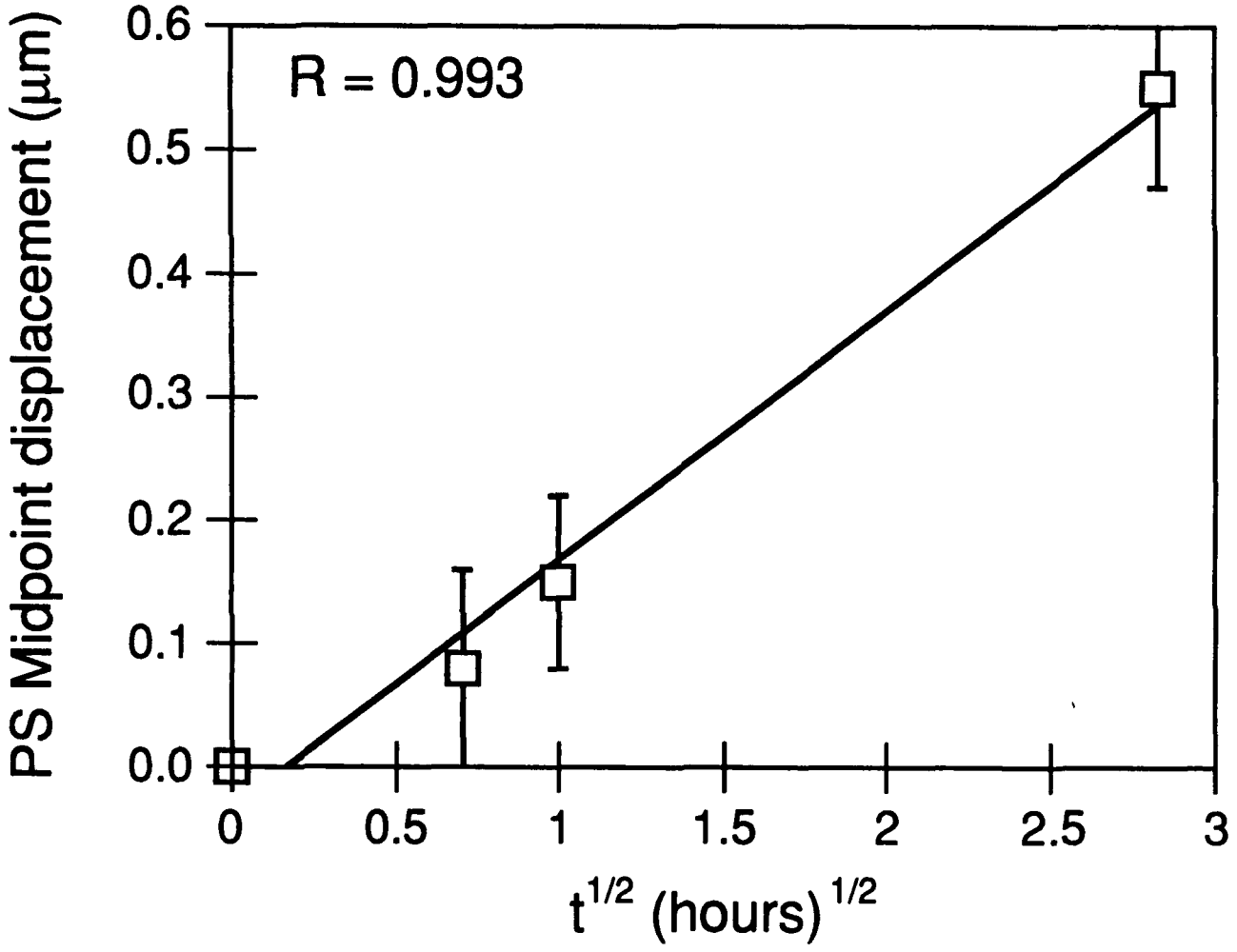
R = 0.993
PS Midpoint displacement (µm)
0.6
0.5
0.4
0.3
0.2
0.1
0.0
0
0.5
1
1.5
2
2.5
3
t^1/2 (hours)^1/2

Figure 13